Dynamic Study of PDT-Induced Oxidative Stress in Cancer Cells Embedded in 3D Collagen Hydrogel Using Genetically Encoded H_2O_2-Sensor

Ludmila M. Sencha, Anastasia A. Gorokhova, Nina N. Peskova, Elena I. Cherkasova, and Irina V. Balalaeva*

Institute of Biology and Biomedicine, Lobachevsky State University of Nizhny Novgorod, 23 Gagarin Ave., Nizhny Novgorod 603950, Russia

* **e-mail:** irin-b@mail.ru

Abstract. Photodynamic therapy (PDT) is a rapidly developing cancer treatment method based on the induction of severe oxidative stress in treated cells. Despite widespread clinical application, the molecular mechanisms underlying the photodynamic reaction have not yet been fully elucidated. Currently, the attention of the scientific community has been drawn to the crucial role of the tumor microenvironment which led to transition from using monolayer cultures of cancer cell to complex 3D *in vitro* models of tumor growth. Such a transition requires modification of existing methods for assessing cellular viability and metabolic responses to therapeutic interventions. We proposed a method for real-time registration of oxidative stress in response to photodynamic therapy in tumor cells embedded in 3D collagen hydrogel. This approach is based on spectroscopic registration of the integral signal from embedded cells expressing genetically encoded fluorescent sensor. The measuring technique does not require the destruction of the hydrogel and allows real-time recording of cell responses to various types of exposure. Using the genetically encoded HyPer sensor, we registered the wave of the secondary production of H_2O_2 in PDT treated cells lasting for about 1–2 h after the end of irradiation and demonstrated it transient mode, which add new information about mechanisms of PDT-induced oxidative stress. We believe that the proposed approach can become a potent and cost-effective option for real-time registration of cells' response to various types of exposure and identification of the underlying mechanisms.

Keywords: photodynamic treatment; hydrogen peroxide; 3D *in vitro* tumor model; collagen hydrogel; protein sensor HyPer; reactive oxygen species; Photosens.

Paper #3566 received 24 Nov 2022; revised manuscript received 6 Dec 2022; accepted for publication 7 Dec 2022; published online 18 Dec 2022. doi: 10.18287/JBPE22.08.040305.

1 Introduction

Photodynamic therapy (PDT) is a potent method of treatment for cancer and some other diseases based on systemic or local administration of a dye, the so-called photosensitizer (PS), and its subsequent activation by light irradiation with a wavelength corresponding to the absorption peak of PS [1]. Activated PS* undergoes inter-system crossing leading to the formation of excited triplet state ^{3}PS* which can enter two types of photochemical reactions. First, due to the long lifetime of the triplet state, ^{3}PS* is able to transfer energy to molecular oxygen (O_2) that is triplet in its ground state. The process of triplet-triplet energy transfer between

^{3}PS* and molecular oxygen with the generation of highly reactive singlet oxygen ($^1O_2$) is called type II photochemical reaction [2, 3]. Type I photochemical reactions include electron and/or proton transfer between triplet-excited PS molecule and molecular oxygen or organic compounds. This process results of generation of radical reactive oxygen species (ROS) [4]. The direct product of electron transfer from PS to oxygen is superoxide radical anion ($O_2^{\bullet-}$); its dismutation or one-electron reduction leads to the production of hydrogen peroxide (H_2O_2); which, in turn, can undergo further reduction to form hydroxyl radicals (HO$^\bullet$) (Haber-Weiss reaction with $O_2^{\bullet-}$ or Fenton reaction with Fe (II)). It is generally accepted that the majority of the PSs used today for PDT realize their activity through type II mechanism. However, both types of photochemical reactions can occur simultaneously with relative contribution depending on the type of PS, oxygen concentration in the tissue, and pH of the medium [5].

All types of photodynamically generated ROS damage most types of biomolecules (amino acids, proteins, lipids, and nucleic acids) eventually leading to the death of cancer cells by apoptosis, autophagy-associated death, or different modalities of necrosis [6]. Photodynamic effect on the tumor and its microenvironment commonly resulted in an acute inflammatory response in the treated area [7, 8]. The development of inflammation stimulates activation of innate immune cells and then forming of adaptive immune response [9]. In later stages, immunological memory may play a key role in the systemic response and may suppress tumor recurrence and spread of metastases in the long term [10]. In the last few decades, PDT has been actively developed and its scope is constantly growing. However, the molecular mechanisms underlying the photodynamic reaction have not yet been fully elucidated. At the same time, the reveling of these mechanisms can provide the basis for rational creation of new compounds and improving the efficiency of photodynamic treatment in clinical oncology.

An obligatory stage during development of drugs and regimens for tumor treatment is their testing on cell cultures *in vitro*. During the last decades, *in vitro* studies were commonly carried out on monolayer cell cultures; however, this model has serious limitations influencing the relevancy of the results. Recently, the attention of the scientific community has been drawn to the crucial role of the tumor microenvironment, which can support tumor cell survival, promotes invasion and metastatic spread of cancer cells, and modulates cell resistance to therapy [11–13]. An important component of tumor microenvironment is extracellular matrix (ECM), since its spatial organization as well as the presence of various active groups can play a significant role in tumor progression [14, 15]. With a growing understanding of the role of the native three-dimensional (3D) tumor microenvironment in tumor development, metastasis, and response to therapeutic interventions, more complex three-dimensional multicomponent cultures are gaining ground. Such models can overcome the limitations of monolayer cell cultures by reproducing the three-dimensional tissue organization and its stiffness, interactions between cells and ECM, gradients of gages, nutrients and metabolites that are characteristic of tumors *in vivo* [16]. It should be especially noted that 3D models demonstrated responses of cancer cells to various therapeutic treatments, which differed significantly from two-dimensional systems [17, 18], in particular, in response to photodynamic exposure [19, 20].

For a successful transition from monolayer to 3D models of tumor growth, it is necessary to modify the methods used to study the effectiveness of anticancer drugs. The measuring techniques must fulfill the requirements of being highly informative and reproducible with low resource consumption, and ensuring dynamic observations of the cell culture growth in a 3D model under physiological conditions. One of the promising approaches for studying cell culture development in a 3D system is the technology of genetic fluorescent labeling of cancer cells [21].

To the moment, multiple fluorescent proteins are available, including those with high sensitivity to physical-chemical parameters of the environment. Thus, H_2O_2-sensitive proteins of HyPer family became a good alternative to the low molecular weight probes for this ROS. The traditional methods for measuring the H_2O_2 based on fluorescent probes (Amplex Red, DCFH-DA, Peroxy Green, etc.), as well as spectrophotometric methods using ferrithiocyanate, tetramethylbenzidine or xylenol orange have the common limitations as a result of their low specificity as well as inability of recording transient changes in the ROS level due to irreversible chemical reaction [22]. HyPer is the first fluorescent genetically encoded sensor that allows registration of the dynamics changes in H_2O_2 content in a whole organism, individual cells or cell compartments [23]. This protein was created by cyclic permutation of the yellow fluorescent protein (cpYFP) and the fusion of its newly formed C- and N-termini with the H_2O_2-sensitive regulatory domain of the prokaryotic peroxide-specific transcription factor OxyR [24]. An important advantage is that the HyPer oxidation is reversible and specific for H_2O_2, which makes it possible to detect transient changes in the level of this particular ROS in the complex cellular environment.

In this work, we present an approach that allows registration of oxidative stress in HyPer-expressing cells embedded in collagen hydrogel without destroying it. The real-time measuring of relative content of H_2O_2 in cancer cells provided new information on the time pattern of H_2O_2 production in response to photodynamic treatment.

2 Materials and Methods

2.1 Cell Lines

The work was carried out using human epidermoid carcinoma A431 (Russian collection of cell cultures, Moscow, Russia) and its derivative line A431-HyPer [25]

stably expressing fluorescent H_2O_2-sensor HyPer [23]. Cells were cultivated on Dulbecco's Modified Eagle's medium (DMEM, PanEco, Russia) containing 2 mM glutamine (PanEco, Moscow, Russia), 10% (v/v) fetal bovine serum (HyClone, Logan, UT, USA), 50 μg/mL penicillin and 50 μg/mL streptomycin (PanEco, Moscow, Russia) at 37 °C in 5% CO_2 atmosphere. For passage, the cells were carefully detached with a trypsin-EDTA solution.

2.2 Production of Collagen Hydrogel-Based 3D Tumor Model

A solution of collagen type I was first prepared according to the previously published protocol from rat tails and stored in sterile 0.1% acetic acid at a final collagen concentration of about 1.2 mg/mL at 4 °C [26]. Sterile stock solutions were precooled to 4 °C in order to prevent fast gelation and then used to prepare a mixture (Mix1) containing 10× DMEM (Biowest, Nuaillé, France), 25 mM glutamine (PanEco, Moscow, Russia), 1M HEPES (PanEco, Moscow, Russia), and 50% fetal bovine serum (HyClone, Logan, UT, USA). Collagen hydrogels were obtained in separate wells of 12- or 24-well plates for tissue cultures (Corning, New York, NY, USA) by thorough mixing of 800 μL of cooled collagen solution, 225 μL of Mix1, 2×10^5 cells for 12-well plate or 1.2×10^6 cells for 24-well plate in 100 μL of DMEM, and 67 μL of 0.34 M NaOH. The gels were incubated at 37 °C in 5% CO_2 for 15–20 min until complete gelation. After solidification of the hydrogel, 1 mL of full serum-supplied DMEM was added to the wells and the hydrogels were separated from the walls of the plate wells.

The resulting hydrogels with embedded cells were incubated at 37 °C in 5% CO_2; the growth medium was changed daily to a fresh medium.

For microscopic analysis, hydrogels were removed from the wells of the plate and imaged with an Olympus X71 inverted microscope with an CPlanFN L 10× / 0.3 objective lens (Olympus, Tokio, Japan) focusing on fixed gel depths.

The diameter of hydrogels was measured by imaging them using DVS-03 whole-body imager (Institute of Photonic Technologies of the Russian Academy of Sciences, Moscow, Russia) followed by image analysis using ImageJ software (version 1.50i, National Institute of Health, USA). For estimation of the gel thickness, the formed hydrogels were removed from the wells of the plate and the thickness was measured by vernier caliper.

2.3 Analysis of Cancer Cell Growth in Collagen Hydrogels by Cell Counting

To assess the rate of cell growth in a 3D model by cell counting, collagen hydrogels were subjected to enzymatic destruction. The hydrogel was placed in a serum-free DMEM medium containing 0.08% collagenase type I (Gibco, New York, NY, USA) and 0.02% trypsin (PanEco, Moscow, Russia) for 1 h at 37 °C. The ratio of gel-to-media volumes was 5:8. After enzymatic destruction of hydrogels, 0.1 mL of 2% trypan blue solution (Sigma-Aldrich, Prague, Czech Republic) was added to the suspension of cells obtained, vortexed, and after 5 min the number of live and dead cells was counted using a hemocytometer. To plot the growth curves of cell cultures in collagen hydrogels, the number of cells was counted in three separate gels every day for 10 days.

2.4 Evaluation of Cancer Cell Growth in Collagen Hydrogels Using Total DNA Measurement

The hydrogels were subjected to enzymatic destruction as described in Section 2.3. After obtaining the cell suspension, the cellular pellet was separated from hydrolyzed collagen by centrifugation at 400 g for 10 min. The total DNA was isolated using the ExtractDNA Blood DNA purification kit (VM011, Eurogen, Moscow, Russia) according to the manufacturer's instructions. The concentration of dissolved DNA was measured on a NanoVue droplet spectrophotometer (GE Healthcare, Fairfield, CT, USA). To plot the growth curves of cell cultures in collagen hydrogels, the amount of total DNA was measured in three separate gels every day for 10 days.

2.5 Cytotoxicity Assay of Photosens against Monolayer Culture

Cells were seeded onto a 96-well plate at concentration of 4×10^3 cells per well and let attach overnight in CO_2 incubator. Then the medium was exchanged to a serum-free medium containing Photosens (PhS) (NIOPIK, Russia) [27], and the cells were incubated for 4 h. The medium was then exchanged with a complete medium without PhS. Photodynamic activity assessment was performed as follows: cells were irradiated using a 655–675 nm LED light source for 96-well plates immediately after the end of incubation with PhS, in a temperature-controlled conditions (37 ºC) [28]. The radiation dose was of 20 J/cm^2 at a constant power density of 32 mW/cm^2. Twenty four h after irradiation of the cells, the complete medium was exchanged with a serum-free medium containing 0.5 mg/ml of MTT reagent (Alfa Aesar, UK), and the cells were incubated for 4 h. Then the medium was aspirated and formed formazan crystals were dissolved in 200 μl of DMSO (PanEco, Russia). The optical density was measured at 570 nm using a Synergy MX microplate reader (BioTek, USA). The relative cell viability was calculated as the percentage of mean optical density in the wells with cells treated with PhS to the mean optical density in the wells with untreated cells. The half-maximal inhibitory concentration (IC_{50}) was calculated using GraphPad Prism software (GraphPad Software, version 6.0 for Windows, San Diego, CA, USA, 2012).

2.6 Monitoring of Hydrogen Peroxide Production in Collagen Hydrogels

To study the response of A431-HyPer cells growing in collagen gels to the addition of H_2O_2 to the cell medium, collagen hydrogels were prepared in 24-well plate as described in Section 2.2. The prepared hydrogels were left overnight in a CO_2 incubator. The medium was then changed to complete medium with 10% FBS. A change in the shape of the HyPer fluorescence excitation spectrum was induced by adding H_2O_2 to the cell medium to a final concentration of 15 μM.

To study the response of A431-HyPer cells in collagen gels to photodynamic treatment, the prepared collagen gels were incubated in a CO_2 incubator for 12 h. Then the medium was changed to a serum-free medium with the addition of PhS at a concentration of 1.5×10^{-8} M and the gels were incubated for 4 h. The medium was then changed to complete growth medium. After that, the hydrogels with cells were irradiated using a LED light source as described above for monolayer culture (Section 2.5).

The excitation and emission fluorescence spectra of the cell-embedded hydrogels were recorded using a Synergy Mx plate reader (BioTek, Vermont, VA, USA) in bottom recording mode. At this mode, the light source irradiates the plate from the bottom side and reflected fluorescence is registered from the same side. The emission of HyPer was excited at 480 nm and recorded in the range of 500–750 nm (Gen5 software, BioTek, Winooski, VT, USA). Fluorescence excitation was performed in the range from 350 to 510 nm, and the signal was recorded at 530 nm. The spectrum registered for 'blank' hydrogel without cells was subtracted for further processing. Then, the ratio I_{500}/I_{420} was calculated by dividing the signals at excitation at 500 nm and 420 nm.

3 Results

3.1 Characterization of A431 Cell Growth in 3D Collagen Hydrogels

To create a three-dimensional model of tumor growth, we chose the A431 human epidermoid carcinoma cell line, since photodynamic therapy is commonly used to treat skin cancer. The collagen hydrogels with diameter of about 20 mm and thickness of about 3 mm were produced using 12-well plate with cells evenly distributed in the gel volume due to production procedure. A431 cells were embedded in collagen hydrogels at a concentration of 2×10^5 cells/gel that was chosen in the course of preliminary experiments. The main criterion for choosing cell seeding density was the growth of the cell culture without a long lag-period or rapid degradation.

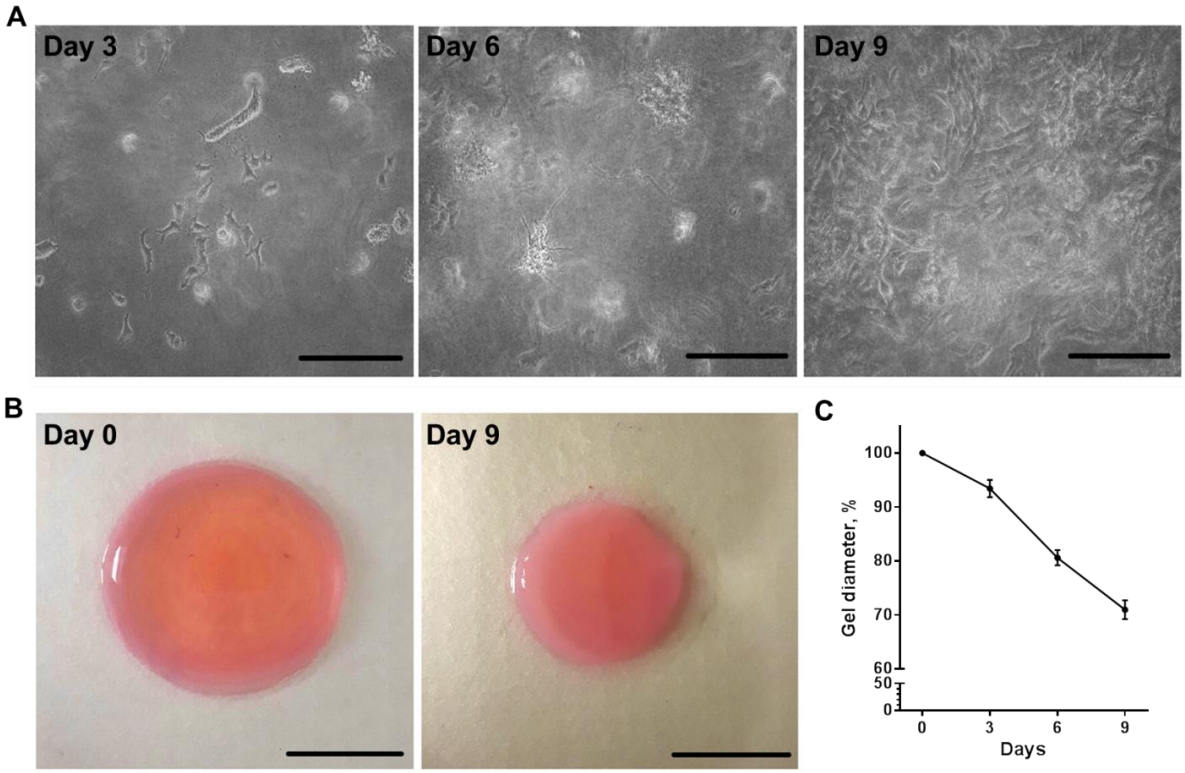

Fig. 1 Growth dynamics of the A431 cells embedded in collagen hydrogels. (A) Microscopic images of cell morphology and distribution in collagen on days 3, 6, and 9 after seeding in hydrogel. The images were obtained at the depth of about 2 mm from the gel bottom side. Scale bar, 100 μm. (B) The images of the collagen gels taken out from the wells of a 12-well plate on day 0 (the day when the cells were embedded in the hydrogel) and on day 9. Scale bar, 10 mm. (C) The contraction of the collagen hydrogels during growth of the embedded cells. Mean ± standard deviation are presented (n = 3).

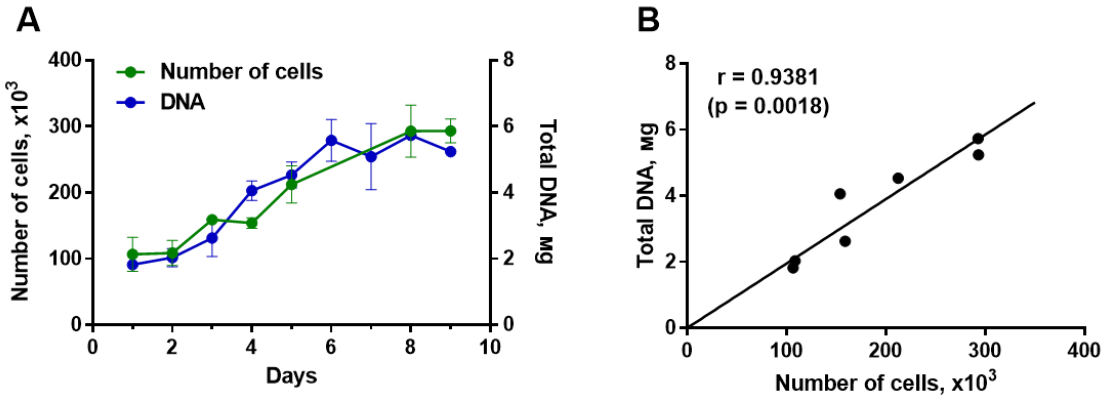

Fig. 2 Analysis of A431 cells growth in collagen hydrogel. (A) Growth curves plotted based on the cells number and total DNA content. Data are presented as mean ± SD (n = 3) (B) Correlation between the results of two methods for cell growth analysis. Pearson correlation coefficient (r) with significance level (p) are presented.

Microscopic examination of cancer cells embedded in the hydrogel showed that the cells begin spreading in the matrix and acquiring an elongated shape by the 3rd day of the experiment (Fig. 1A). Later, the cells form clusters, followed by the formation of a dense 3D network of cell strands in the gel volume, which is clearly visible on the 9th day of the experiment. An increase in the cell number and the formation of elongated cell strands were accompanied by pronounced change in the size of the gel (Fig. 1B, C). During the entire period of cell cultivation, a gradual contraction of the gels was observed, which reached a maximum on the 9th day of observation and amounted to about 30% of the initial diameter. This phenomenon was previously documented for cells of various origins cultured in collagen and is considered to be a consequence of the ability of cells to enzymatically destroy and/or remodel the matrix [29].

To quantify the growth of A431 cells in collagen hydrogels, two methods were applied. First, the cells were isolated from the gel volume and counted; second, we measured the total DNA content at different days of the culture development. The resulting growth curves demonstrate a gradual increase in the number of cells by 2.7 times during 9 days of cultivation. Very similar results were obtained for DNA analysis with increase by 2.8 times over the period of the experiment (Fig. 2A). The strong correlation between the results (the Pearson correlation coefficient is 0.9381; $p = 0.0018$) demonstrated high level of agreement of two methods (Fig. 2B).

It should be noted that the growth rate of A431 cell in 3D collagen hydrogel is lower than that for the A431 cell line in monolayer culture, where the cell doubling period is about 26 h [30]. This can be due to interaction of the cells in 3D model with the surrounding collagen matrix, which prevents them from growing freely. In addition, similarly to *in vivo* conditions, there is a nutrient gradient in such a system, which also can affect the cell growth [16].

3.2 Photodynamic Activity of Photosens against A431 Cells

The response of cells to photodynamic exposure was studied using Photosens, which belongs to the group of phthalocyanines and is a mixture of di-, tri-, and tetrasubstituted fractions of aluminum phthalocyanine with the number of sulfo groups of 3.4 [27, 31].

A dose-dependent decrease in the viability of A431 cells was shown after treatment with Photosens in the concentration range of 10^{-9}–10^{-4} M and irradiation dose of 20 J/cm^2 at 655–675 nm (Fig. 3). The calculated value of IC_{50} under the chosen irradiation conditions was 1.5×10^{-8} M. At the same time, the dark toxicity of this compound (in the absence of irradiation) was more than 100 μM, which exceeds that under irradiation by at least 4 orders of magnitude. Based on the obtained results, the concentration of the photosensitizer corresponding to the IC_{50} (1.5×10^{-8} M) was chosen for further work.

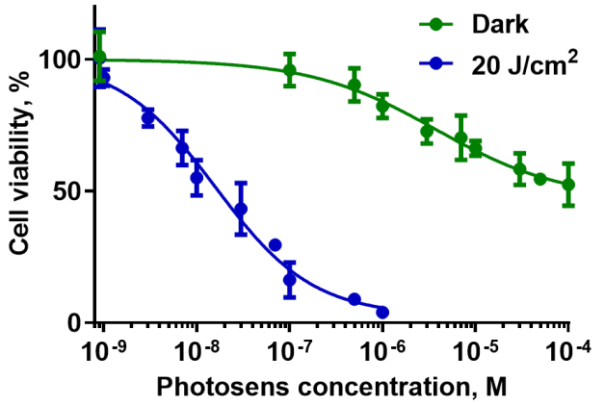

Fig. 3 Dark toxicity and photodynamic activity of Photosens against the A431 cell line, measured by MTT assay. Cells were incubated with the photosensitizer for 4 h followed by the medium exchange. To induce a photodynamic response, cells were irradiated with light in the range of 655–675 nm at a dose of 20 J/cm^2 and a constant power density of 32 mW/cm^2. Cell viability was assessed 24 h after irradiation. Data are represented as mean ± SD (n = 3).

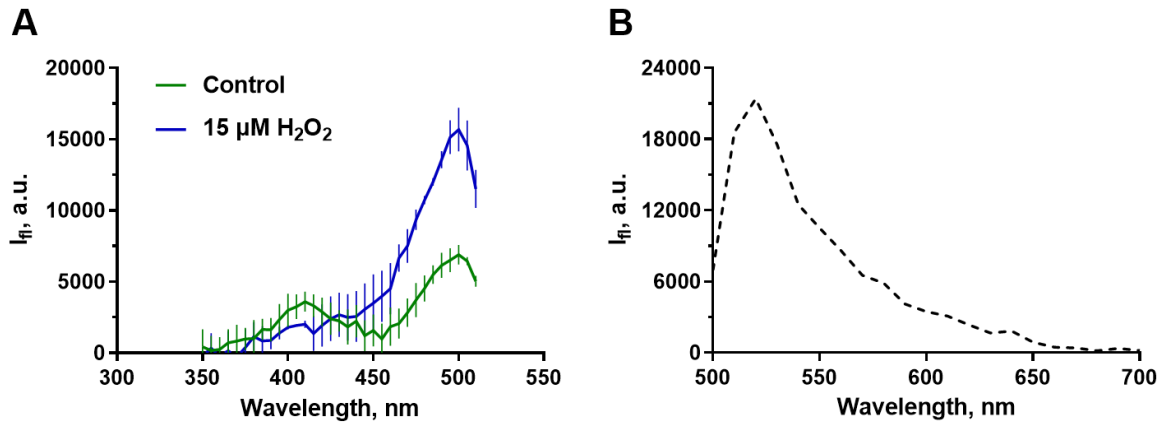

Fig. 4 Fluorescence excitation spectrum of A431-HyPer cells in collagen matrices before (control) and 1 h after addition of 15 μM H_2O_2 (A); and fluorescence emission spectrum of the 3D cell culture (B).

3.3 Study of Oxidation Stress in Collagen Hydrogels-Based Model of Tumor Growth Using an H_2O_2-Responsive Sensor Hyper

To detect the response of cells to oxidative stress, we used an approach based on the spectroscopic registration of the integral fluorescent signal from cell-embedded hydrogels. In this part of work, the 24-well plates were used for gels production with gel diameter of 15 mm and thickness of 5 mm. The excitation and fluorescence emission spectra of the whole matrices, without their destruction, were analyzed using a plate reader. It should be noted that this approach cannot be implemented for a monolayer cell culture, but it becomes possible due to the peculiarities of the optical properties of the matrices. When working with a monolayer culture, cells located in a thin layer of ~ 1–3 μm do not allow reliable recording of the fluorescence signal when detecting transmitted light; similarly, a low level of scattering does not allow detecting reflected light. In a collagen hydrogel of 5 mm thickness, the number of cells per well area is 10–12 times higher than that in a monolayer. Most importantly, strong light scattering in the gel provides a high level of fluorescence signal recorded in reflection mode. This approach makes it possible to record the signal from the native hydrogel without destroying it or compromising the sterility of the cultivation conditions.

An additional advantage of non-destructive monitoring of the cells in the hydrogel is the ability to register a signal from genetically encoded sensors in real time, thus monitoring the response of cells to various factors. Using this approach, we confirmed the sensitivity of A431-HyPer cells to a model stimulus, namely, the addition of hydrogen peroxide to the medium.

It was shown that A431-HyPer cells grown in a hydrogel respond to exogenous H_2O_2 in an expected manner. One hour after addition of H_2O_2 to the medium to a concentration of 15 μM, a clearly noticeable change in the shape of the excitation spectrum occurs: a decrease in the excitation peak at 420 nm and an increase at 500 nm (Fig. 4A). At the same time, the fluorescence spectrum retains the shape characteristic of this protein (Fig. 4B).

3.4 Dynamic Study of Oxidative Stress Development in Response to Photodynamic Treatment

The development of oxidative stress is a key step in the response of cancer cells to photodynamic treatment. In this case, the dynamics of primary and secondary ROS production after the cell irradiation plays an important role. Using the proposed approach, we studied the change in the concentration of H_2O_2 in A431-HyPer cells under photodynamic exposure with Photosens. Oxidative stress was registered in cells embedded in collagen matrices.

Irradiation of the Photosens pre-treated hydrogels at a dose of 20 J/cm^2 led to a pronounced change in the shape of the HyPer fluorescence excitation spectrum (Fig. 5A). To analyze the dynamics of the developing response, we used the ratiometric index I_{500}/I_{420}, calculated as the ratio of the fluorescence intensity upon excitation at the corresponding wavelengths. According to the results obtained, the I_{500}/I_{420} index consistently increased and reached its maximum 60 min after the photodynamic exposure, exceeding the initial values by 1.8 times (Fig. 5B). However, after reaching the peak, the I_{500}/I_{420} index gradually decreased to the initial level, which suggests a transient increase in the content of hydrogen peroxide in irradiated PhS-treated cells. It should be noted separately that an increase in the H_2O_2 content was recorded for a relatively long time after the end of irradiation, under the conditions of the impossibility of continuing photochemical reactions with participation of the photosensitizer. This allows us to state about H_2O_2 production in the course of secondary processes developing as a result of photodynamic action.

4 Discussion

Oxidative stress is a condition characterized by an excessive ROS generation in cells outrunning their scavenging by antioxidant system [32].

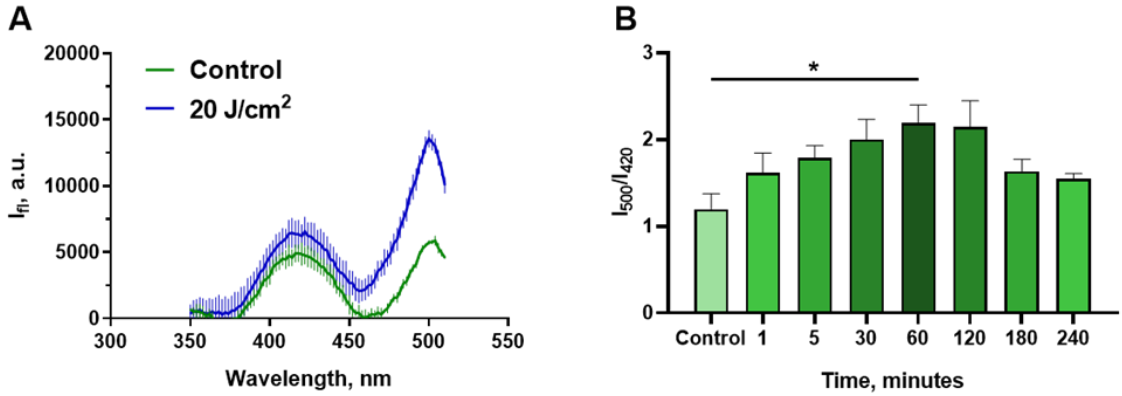

Fig. 5 Development of oxidative stress in A431-HyPer cells embedded in collagen matrices in response to photodynamic treatment with Photosens at a concentration of 1.5×10^{-8} M, irradiation at a dose of 20 J/cm^2, and a constant power density of 32 mW/cm^2. (A) Fluorescence excitation spectrum of hydrogels with A431-HyPer cells before (control) and 1 h after photodynamic exposure. (B) Dynamics of the I_{500} / I_{420} index of HyPer fluorescence at different time points after photodynamic treatment of the hydrogels. * – indicates significant difference from control (Dunnett multiple comparisons test, $p < 0.05$). Data are presented as mean ± SD (n = 3).

The physiological amount of ROS plays an important role in the cell vitality, but when the ROS level is abnormally elevated, it can cause irreversible cell damage. The cytotoxic effect of ROS results from the oxidation of cellular macromolecules such as lipids, proteins and nucleic acids, damage to membrane structures and supramolecular complexes [33]. It is commonly accepted, that singlet oxygen $^1O_2$ is the first echelon and the main cytotoxic ROS produced in the course of PDT [34]. However, many evidences are accumulated about an increased production or accumulation of other ROS under photodynamic treatment: hydroxyl radical [35], hydrogen peroxide [25], nitric oxide [36], and others. It should be noted that almost all of these cytotoxic agents have very short lifetime. Notwithstanding, it is clearly proven that PDT can cause long-term oxidative stress in cells [37, 38]. The long-lasting oxidative conditions after the end of light irradiation can be potentially initiated by hydrogen peroxide [39], which is relatively stable (half-life is about 1 ms) and can participate in reactions with biomolecules at a considerable distance from the sites of its formation [40]. H_2O_2 is able to act as an extracellular and intracellular signaling molecule that mediates multiple effects in biological systems [32]. Targets of H_2O_2-mediated oxidation are thiol groups of peroxiredoxins and other cysteine-containing proteins [41, 42]. Hydrogen peroxide oxidizes the phosphatases catalytic cysteine of mitogen-activated protein kinases (MAPK) and inactivates them thereby activating c-Jun N-terminal kinases (JNK) and p38 MAPK. H_2O_2-dependent activation JNK can induce the development of apoptosis or trigger necrotic cell death [43]. Moreover, JNK is able to influence the activity of many mitochondrial and nuclear proteins, thereby regulating cell growth, migration, proliferation, and cell survival [44]. Additionally, H_2O_2-dependent activation of p38 MAPK, in turn, activates the transcription factor NF-κB, which may affect the survival and metastasis of cancer cells [45]. Thus, H_2O_2 can both control intracellular signal transduction and promote tissue response [46].

In addition to its important role in cellular signaling, an excess of H_2O_2 can act as a major precursor for other highly active ROS, such as hydroxyl radical, peroxynitrite, and hydrochlorides. Oxidation of biologically important substrates causes an imbalance in the physiological redox state of cells, leading to the development of oxidative stress and cell death in one of the ways: apoptosis, autophagy, or various modalities of necrosis in case of a high level of damage [47, 48].

We have previously experimentally demonstrated the great opportunities provided by real-time monitoring of H_2O_2 production in a monolayer cell culture after photodynamic treatment using confocal microscopy [25, 49]. However, this approach is not suitable for 3D models of tumor growth as it has a very low penetration depth. In this work, we propose an approach that makes it possible to record the integral fluorescence signal from hydrogels with embedded cells using the spectroscopic method. For registration of H_2O_2 content, a genetically encoded HyPer fluorescent sensor was used. Unlike low molecular weight probes, HyPer is characterized by high selectivity (it does not react to other types of ROS) and sensitivity to hydrogen peroxide, showing a high affinity for H_2O_2 at submicromolar concentrations [23]. An ability to apply a ratiometric registration provide stable results in a complex cellular media with unknown local concentrations of the sensor. Moreover, HyPer reaction with H_2O_2 is reversible, which makes it possible to observe the dynamics of H_2O_2 accumulation and restoration in living systems in real time.

The peculiarities of the structure and optical properties of matrices, such as a high level of scattering along with a low level of absorption in the visible range,

allowed us to analyze the excitation and fluorescence emission spectra of the whole collagen hydrogels using a plate reader. This approach, firstly, makes it possible to record the response from a three-dimensional system without destroying it or violating the sterility of cultivation conditions. Secondly, it significantly reduces the resource consumption of the study, as well as its laboriousness. And thirdly, an important advantage is the ability to register a signal from genetically encoded sensors in real time in physiological conditions, monitoring the metabolic changes in cells in response to the action of various factors. Since the proposed technique was applied to collagen hydrogels, we believe that it can be used for hydrogels prepared from multiple other types of polymers suitable for tissue engineering. The list of potentially applicable polymers includes alginate, fibrin, gelatin, methylcellulose, Matrigel™, modified hyaluronic acid, etc. [50–52]. The crucial factors will be the combination of low light absorption in the region of the fluorescent protein excitation and emission with relatively high light scattering.

Using the proposed approach, we have shown a gradual increase in the content of H_2O_2 in a three-dimensional model of tumor growth within 1 h after photodynamic therapy. The response for such a long time after the end of irradiation cannot be considered as a continuation of photochemical reactions with participation of the photosensitizer. We believe that the production of H_2O_2 occurs in the course of secondary "dark" processes that develop as a result of the primary photodynamic effect. To date, a few evidences of secondary ROS production has been published, which is recorded after the completion of irradiation and is a consequence of the damage to the mitochondrial electron transport chains and depletion of the antioxidant defense system [53, 54]. The results obtained on the 3D model are consistent with the behavior of cells in a monolayer culture [25]. We also showed for the first time the reversibility of this reaction, which indicates the transient increase in the content of H_2O_2 in cells, the phenomenon, which cannot be established using low molecular weight probes for hydrogen peroxide. Obviously, photodynamic therapy triggers the formation of not only primary, but also secondary wave of ROS production. However, the detailed mechanisms of this phenomenon require further investigation.

5 Conclusion

Development and broad implementation of 3D *in vitro* tumor models offer more and more opportunities for studying the molecular and cellular mechanisms of tumor growth, as well as drug screening and testing. Complex spatial structure of 3D models necessitates the creation of new methodological approaches for cell studies. We have proposed a technique for real-time registration of oxidative stress in response to photodynamic therapy in tumor cells embedded in collagen hydrogel. This approach does not require the destruction of hydrogel and significantly reduces the cost of research. Using the genetically encoded HyPer sensor, we registered the transient wave of the secondary production of H_2O_2 in PDT treated cells, which add new information about molecular mechanisms of oxidative stress. We believe that the proposed approach can become a potent and cost-effective option for real-time registration of cells' response to various types of exposure and identification of the underlying mechanisms.

Disclosures

The authors declare no conflict of interest.

6 Acknowledgements

This research was supported by Center of Excellence "Center of Photonics" funded by The Ministry of Science and Higher Education of the Russian Federation, contract No 075-15-2022-293. Authors thank O. E. Dobrynina for the invaluable help in carrying out the experiments.

References

1. D. V. Straten, V. Mashayekhi, H. S. De Bruijn, S. Oliveira, and D. J. Robinson, "Oncologic Photodynamic Therapy: Basic Principles, Current Clinical Status and Future Directions," Cancers 9(2), 19 (2017).
2. A. B. Uzdensky, "The biophysical aspects of photodynamic therapy," Biophysics 61, 461–469 (2016).
3. S. Kwiatkowski, "Photodynamic therapy–mechanisms, photosensitizers and combinations," Biomedicine & Pharmacotherapy 106, 1098–1107 (2018).
4. Z. Zhou, "Reactive oxygen species generating systems meeting challenges of photodynamic cancer therapy," Chemical Society Reviews 45, 6597–6626 (2016).
5. M. S. Baptista, J. Cadet, P. Di Mascio, A. A. Ghogare, A. Greer, M. R. Hamblin, C. Lorente, S. C. Nunez, M. S. Ribeiro, A. H. Thomas, and M. Vignoni, "Type I and type II photosensitized oxidation reactions: guidelines and mechanistic pathways," Photochemistry and Photobiology 93, 912–919 (2017).
6. A. M. Ibarra, R. B. Cecatto, L. J. Motta, A. L. dos Santos Franco, D. de Fátima Teixeira da Silva, F. D. Nunes, M. R. Hamblin, and M. F. Rodrigues, "Photodynamic therapy for squamous cell carcinoma of the head and neck: narrative review focusing on photosensitizers," Lasers in Medical Science 37, 1441–1470 (2021).
7. E. Reginato, P. Wolf, and M. R. Hamblin, "Immune response after photodynamic therapy increases anti-cancer and anti-bacterial effects," World Journal of Immunology 4(1), (2014).

8. Y. Yang, Y. Hu, and H. Wang, "Targeting antitumor immune response for enhancing the efficacy of photodynamic therapy of cancer: recent advances and future perspectives," Oxidative Medicine and Cellular Longevity 2016, 5274084 (2016).
9. I. Beltrán Hernández, Y. Yu, F. Ossendorp, M. Korbelik, and S. Oliveira, "Preclinical and clinical evidence of immune responses triggered in oncologic photodynamic therapy: clinical recommendations," Journal of Clinical Medicine 9(2), (2020).
10. N. W. Nkune, N. W. Simelane, H. Montaseri, and H. Abrahamse, "Photodynamic Therapy-Mediated Immune Responses in Three-Dimensional Tumor Models," International Journal of Molecular Sciences 22(23), 12618 (2021).
11. M. W. Pickup, J. K. Mouw, and V. M. Weaver, "The extracellular matrix modulates the hallmarks of cancer," EMBO Reports 15(12), 1243–1253 (2014).
12. C. Walker, E. Mojares, and A. del Río Hernández, "Role of extracellular matrix in development and cancer progression," International Journal of Molecular Sciences 19(10), 3028 (2018).
13. C. Frantz, K. M. Stewart, and V. M. Weaver, "The extracellular matrix at a glance," Journal of Cell Science 123(24), 4195–4200 (2010).
14. J. M. Northcott, I. S. Dean, J. K. Mouw, and V. M. Weaver, "Feeling stress: the mechanics of cancer progression and aggression," Frontiers in Cell and Developmental Biology 6, 17 (2018).
15. S. H. Kim, J. Turnbull, and S. Guimond, "Extracellular matrix and cell signalling: the dynamic cooperation of integrin, proteoglycan and growth factor receptor," The Journal of Endocrinology 209(2), 139–151 (2011).
16. K. Duval, H. Grover, L. H. Han, Y. Mou, A. F. Pegoraro, J. Fredberg, and Z. Chen, "Modeling physiological events in 2D vs. 3D cell culture," Physiology 32(4), 266–277 (2017).
17. O. M. Kutova, L. M. Sencha, A. D. Pospelov, O. E. Dobrynina, A. A. Brilkina, E. I. Cherkasova, and I. V. Balalaeva, "Comparative analysis of cell–cell contact abundance in ovarian carcinoma cells cultured in two-and three-dimensional in vitro models," Biology 9(2), 446 (2020).
18. S. Breslin, L. O'Driscoll, "Three-dimensional cell culture: the missing link in drug discovery," Drug Discovery Today 18, 240–249 (2013).
19. E. A. Sokolova, A. O. Senatskaya, S. A. Lermontova, E. K. Akinchits, L. G. Klapshina, A. A. Brilkina, and I. V. Balalaeva, "Model of Ovarian Adenocarcinoma Spheroids for Assessing Photodynamic Cytotoxicity," Modern Technologies in Medicine 12(1), 34–40 (2020).
20. L. Mohammad Hadi, E. Yaghini, A. J. MacRobert, and M. Loizidou, "Synergy between photodynamic therapy and dactinomycin chemotherapy in 2D and 3D ovarian cancer cell cultures," International Journal of Molecular Sciences 21(9), 3203 (2020).
21. D. M. Chudakov, M. V. Matz, S. Lukyanov, and K. A. Lukyanov, "Fluorescent proteins and their applications in imaging living cells and tissues," Physiological Reviews 90(3), 1103–1163 (2010).
22. S. G. Rhee, T. S. Chang, W. Jeong, and D. Kang, "Methods for detection and measurement of hydrogen peroxide inside and outside of cells," Molecules and Cells 29, 539–549 (2010).
23. V. V. Belousov, A. F. Fradkov, K. A. Lukyanov, D. B. Staroverov, K. S. Shakhbazov, A. V. Terskikh, and S. Lukyanov, "Genetically encoded fluorescent indicator for intracellular hydrogen peroxide," Nature Methods 3, 281–286 (2006).
24. H. J. Choi, S. J. Kim, P. Mukhopadhyay, S. Cho, J. R. Woo, G. Storz, and S. E. Ryu, "Structural basis of the redox switch in the OxyR transcription factor," Cell 105(1), 103–113 (2001).
25. N. N. Peskova, A. A. Brilkina, A. A. Gorokhova, N. Y. Shilyagina, O. M. Kutova, A. S. Nerush, A. G. Orlova, L. G. Klapshina, V. V. Vodeneev, and I. V. Balalaeva, "The localization of the photosensitizer determines the dynamics of the secondary production of hydrogen peroxide in cell cytoplasm and mitochondria," Journal of Photochemistry and Photobiology B: Biology 219, 112208 (2021).
26. L. M. Sencha, O. E. Dobrynina, A. D. Pospelov, E. L. Guryev, N. N. Peskova, A. A. Brilkina, E. I. Cherkasova, and I. V. Balalaeva, "Real-Time Fluorescence Visualization and Quantitation of Cell Growth and Death in Response to Treatment in 3D Collagen-Based Tumor Model," International Journal of Molecular Sciences 23(16), 8837 (2022).
27. E. A. Lukyanets, "Phthalocyanines as photosensitizers in the photodynamic therapy of cancer," Journal of Porphyrins and Phthalocyanines 3(6), 424–432 (1999).
28. N. Y. Shilyagina, V. I. Plekhanov, I. V. Shkunov, P. A. Shilyagin, L. V. Dubasova, A. A. Brilkina, E. A. Sokolova, I. V. Turchin, and I. V. Balalaeva, "LED light source for in vitro study of photosensitizing agents for photodynamic therapy," Modern Technologies in Medicine 6(2), 15–22 (2014).
29. C. M. Brougham, T. J. Levingstone, S. Jockenhoevel, T. C. Flanagan, and F. J. O'Brien, "Incorporation of fibrin into a collagen–glycosaminoglycan matrix results in a scaffold with improved mechanical properties and enhanced capacity to resist cell-mediated contraction," Acta Biomaterialia 26(15), 205–214 (2015).
30. S. S. Soroko, L. N. Shestakova, A. A. Brilkina, E. K. Akinchits, V. A. Vodeneev, and N. Y. Shilyagina, "Radiosensitivity of A431, CHO, and SK-BR-3 cell lines to low-intensity beta radiation from a Sr-90+ Y-90 mixed source," Opera Medica et Physiologica 8(1), 37–44 (2021).

31. A. A. Brilkina, L. V. Dubasova, E. A. Sergeeva, A. J. Pospelov, N. Y. Shilyagina, N. M. Shakhova, and I. V. Balalaeva, "Photobiological properties of phthalocyanine photosensitizers Photosens, Holosens and Phthalosens: A comparative in vitro analysis," Journal of Photochemistry and Photobiology B: Biology 191, 128–134 (2019).
32. H. Sies, C. Berndt, and D. P. Jones, "Oxidative stress," Annual Review of Biochemistry 86, 715–748 (2017).
33. S. Kwon, H. Ko, D. G. You, K. Kataoka, and J. H. Park, "Nanomedicines for reactive oxygen species mediated approach: an emerging paradigm for cancer treatment," Accounts of Chemical Research 52(7), 1771–1782 (2019).
34. B. Li, L. Lin, H. Lin, and B. C. Wilson, "Photosensitized singlet oxygen generation and detection: Recent advances and future perspectives in cancer photodynamic therapy," Journal of Biophotonics 9(11–12), 1314–1325 (2016).
35. Y. Choi, J. E. Chang, S. Jheon, S. J. Han, and J. K. Kim, "Enhanced production of reactive oxygen species in HeLa cells under concurrent low-dose carboplatin and Photofrin® photodynamic therapy," Oncology Reports 40(1), 339–345 (2018).
36. N. Nwahara, M. Motaung, G. Abrahams, P. Mashazi, J. Mack, E. Prinsloo, and T. Nyokong, "Dual singlet oxygen and nitric oxide-releasing silicon phthalocyanine for augmented photodynamic therapy," Materials Today Chemistry 26, 101201 (2022).
37. P. Mroz, A. Yaroslavsky, G. B. Kharkwal, and M. R. Hamblin, "Cell death pathways in photodynamic therapy of cancer," Cancers 3(2), 2516–2539 (2011).
38. I. O. Bacellar, T. M. Tsubone, C. Pavani, and M. S. Baptista, "Photodynamic efficiency: from molecular photochemistry to cell death," International Journal of Molecular Sciences 16(9), 20523–20559 (2015).
39. K. Khorsandi, R. Hosseinzadeh R, H. Esfahani H, K. Zandsalimi K, F. K. Shahidi, and H. Abrahamse, "Accelerating skin regeneration and wound healing by controlled ROS from photodynamic treatment," Inflammation and Regeneration 42, 40 (2022).
40. N. Yang, W. Xiao, X. Song, W. Wang, and X. Dong, "Recent advances in tumor microenvironment hydrogen peroxide-responsive materials for cancer photodynamic therapy," Nano-Micro Letters 12, 15 (2020).
41. A. G. Cox, M. B. Hampton, "Bcl-2 over-expression promotes genomic instability by inhibiting apoptosis of cells exposed to hydrogen peroxide," Carcinogenesis 28, 2166–2171 (2007).
42. F. M. Low, M. B. Hampton, A. V. Peskin, and C. C. Winterbourn, "Peroxiredoxin 2 functions as a noncatalytic scavenger of low-level hydrogen peroxide in the erythrocyte," Blood 109(6), 2611–2617 (2007).
43. H. Kamata, S. I. Honda, S. Maeda, L. Chang, H. Hirata, and M. Karin, "Reactive oxygen species promote TNFα-induced death and sustained JNK activation by inhibiting MAP kinase phosphatases," Cell 120(5), 649–661 (2005).
44. C. Song, W. Xu, H. Wu, X. Wang, Q. Gong, C. Liu, J. Liu, and L. Zhou, "Photodynamic therapy induces autophagy-mediated cell death in human colorectal cancer cells via activation of the ROS/JNK signaling pathway," Cell Death & Disease 11, 938 (2020).
45. S. A. Vlahopoulos, "Aberrant control of NF-κB in cancer permits transcriptional and phenotypic plasticity, to curtail dependence on host tissue: molecular mode," Cancer Biology & Medicine 14, 254 (2017).
46. A. A. Gorokhova, Y. S. Bugrova, N. N. Peskova, and I. V. Balalaeva, "Photodynamic Treatment Can Induce Enhanced Generation of Hydrogen Peroxide in Cells Outside the Irradiated Area: Proof of the Phenomenon on Cell Culture in vitro," Opera Medica et Physiologica 8, 15–24 (2021).
47. M. Broekgaarden, R. Weijer, T. M. van Gulik, M. R. Hamblin, and M. Heger, "Tumor cell survival pathways activated by photodynamic therapy: a molecular basis for pharmacological inhibition strategies," Cancer and Metastasis Reviews 34(4), 643–690 (2015).
48. T. Mishchenko, I. Balalaeva, A. Gorokhova, M. Vedunova, and D. V. Krysko, "Which cell death modality wins the contest for photodynamic therapy of cancer?" Cell Death & Disease 13(5), 455 (2022).
49. A. A. Brilkina, N. N. Peskova, V. V. Dudenkova, A. A. Gorokhova, E. A. Sokolova, and I. V. Balalaeva, "Monitoring of hydrogen peroxide production under photodynamic treatment using protein sensor HyPer," Journal of Photochemistry and Photobiology B: Biology 178, 296–301 (2018).
50. J. M. Zuidema, C. J. Rivet, R. J. Gilbert, and F. A. Morrison, "A protocol for rheological characterization of hydrogels for tissue engineering strategies," Journal of Biomedical Materials Research Part B: Applied Biomaterials 102, 1063–1073 (2014).
51. M. C. Catoira, L. Fusaro, D. Di Francesco, M. Ramella, and F. Boccafoschi, "Overview of natural hydrogels for regenerative medicine applications," Journal of Materials Science: Materials in Medicine 30(10), 115 (2019).
52. A. V. Sochilina, A. G. Savelyev, R. A. Akasov, V. P. Zubov, E. V. Khaydukov, and A. N. Generalova, "Preparing Modified Hyaluronic Acid with Tunable Content of Vinyl Groups for Use in Fabrication of Scaffolds by Photoinduced Crosslinking," Russian Journal of Bioorganic Chemistry 47(4), 828–836 (2021).
53. H. Abrahamse, N. N. Houreld, "Genetic aberrations associated with photodynamic therapy in colorectal cancer cells," International Journal of Molecular Sciences 20(13), 3254 (2019).
54. H. Sies, "Hydrogen peroxide as a central redox signaling molecule in physiological oxidative stress: Oxidative eustress," Redox Biology 11, 613–619 (2017).